Remarks on two-pass 3-D migration error

Stewart A. Levin

Introduction

Recently the author has studied errors of a two-pass method for migrating three dimensional stacked data that cascades two dimensional migrations in orthogonal directions [Gibson, Larner, and Levin (1983), Jakubowicz and Levin (1983)]. For constant velocity migration errors arise only from approximations to the complete migration operator provided by the scalar wave equation. When the 90° Stolt migration algorithm is used the results match full 3-D Stolt migration exactly. For nonconstant velocity media the method is necessarily approximate because its 2-D migration velocities are tied to a local, partially migrated position rather than the final (out of plane) position that is the apex of a full 3-D migration hyperboloid. For a reasonably large range of dips and velocity functions, numerical simulation showed errors of the same order as that which normally arises from velocity uncertainty. In the latter half of this note we will argue that these errors are virtually identical to those incurred by using Stolt's trace stretching trick for handling nonconstant velocity.

Jakubowicz and Levin (1983) give an example comparing the errors of *continuous* 15° full versus two-pass constant velocity migration. Mention is also made of discrete implementation errors but no example is shown. The next section will briefly discuss how to measure this error and supply some examples.

Discrete two-pass 15° error

If we measure all times and distances as multiples of the basic sampling intervals Δt and Δx, the phase shift k_τ for 15° time domain migration as a function of normalized frequency ω, spatial wavenumber k_x and downward extrapolation traveltime step $\Delta\tau$ is given implicitly by the all pass transfer function

$$e^{i\Delta\tau(k_\tau-\omega)} = -\frac{\gamma(k_x)\,e^{i\omega}+1}{e^{i\omega}+\gamma(k_x)} \tag{1}$$

where, for the explicit algorithm, γ takes the form

$$2A\,V^2(\cos k_x - 1) - 1 \quad , \tag{2a}$$

while for the implicit algorithm the expression is

$$\frac{(2A\,V^2 - 2\beta)(\cos k_x - 1) - 1}{(2A\,V^2 + 2\beta)(\cos k_x - 1) + 1} \quad . \tag{2b}$$

Here A is $\Delta\tau/32$, and β is typically 1/6.

Applying this to two-pass migration, where we do an x-migration followed by a y-migration, k_τ is given by

$$e^{i\Delta\tau(k_\tau - \omega')} \;=\; -\,\frac{\gamma(k_y)\,e^{i\omega'} + 1}{e^{i\omega'} + \gamma(k_y)} \quad , \tag{3a}$$

where

$$e^{i\Delta\tau(\omega' - \omega)} \;=\; -\,\frac{\gamma(k_x)\,e^{i\omega} + 1}{e^{i\omega} + \gamma(k_x)} \quad . \tag{3b}$$

To compute k_τ for one-pass discrete 3-D migration, unlike the continuous case discussed by Brown (1983), it makes a difference whether or not the extrapolation operator is split. It is customary to split an extrapolation operator into two orthogonal parts - each being the operator used for two dimensional migration. We will use this scheme in our examples. (This is not the only splitting possible. Four second order operators oriented at 45° angles can been used for greater accuracy.) With this assumption, the transfer function for one-step migration is

$$e^{i\Delta\tau(k_\tau - \omega)} \;=\; \frac{\gamma(k_x)\,e^{i\omega} + 1}{e^{i\omega} + \gamma(k_x)} \cdot \frac{\gamma(k_y)\,e^{i\omega} + 1}{e^{i\omega} + \gamma(k_y)} \quad . \tag{4}$$

To now compare one- and two-pass 15° migration error we use formulas (3) and (4) to compute relative phase error

$$\frac{k_\tau}{\omega\cos\theta} - 1 \quad . \tag{5}$$

(For a given subsurface dip θ, the phase shift k_τ of 90° migration is $\omega\cos\theta$.) It is meaningful to plot this as a function of dip angle θ and azimuth α because

$$\frac{V k_x}{2\omega} \;=\; \cos\alpha\,\sin\theta \tag{6a}$$

and

$$\frac{V k_y}{2\omega} = \sin\alpha \sin\theta \quad . \tag{6b}$$

These formulas were used to generate the sample data contoured in Figures 1 and 2. Figure 1 shows phase error plots that are virtually identical, typical behavior in all the explicit 15° algorithm test made. Both show a slight *increase* in accuracy around 45° azimuth, just as the two-pass method did in the continuous case and for essentially the same reason. Figure 2 shows the same test switching to the implicit 15° algorithm. They too are representative of most other implicit phase error plots we generated. Here the phase error, unlike the continuous case, goes negative in places. Furthermore we see the two-pass error is not guaranteed to be minimized around 45° azimuth but may even be maximized over some range of dip.

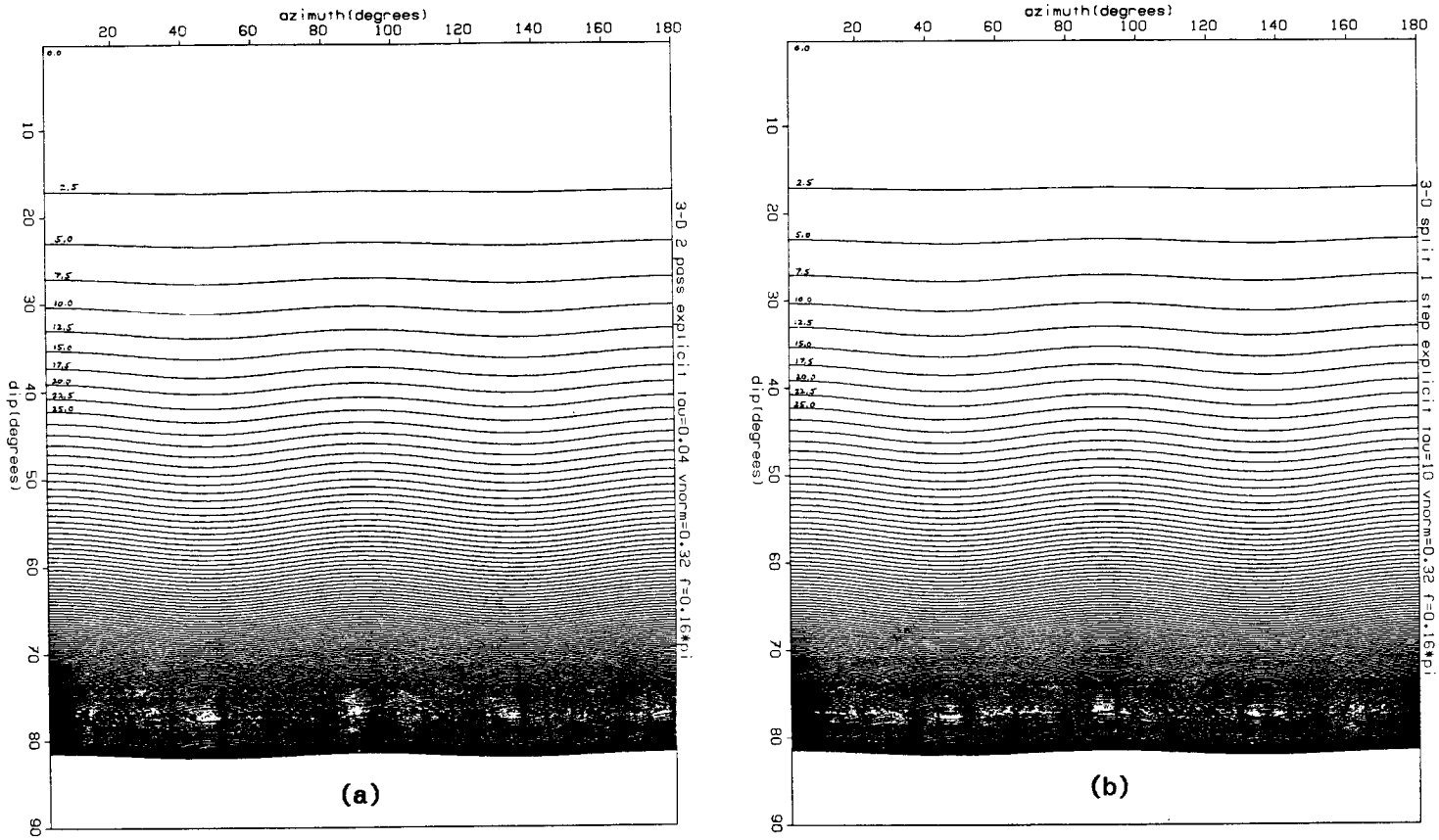

FIG. 1. Contour plot of relative phase error for (a) two-pass 15° explicit 3-D migration and (b) full 15° explicit split step 3-D migration. Velocity here is 4000 m/sec and frequency 20 Hz at a 4 msec sampling rate. A downward continuation step size of 40 msec and a trace spacing of 50 m are also assumed. Contour interval is 2½% with zero error along the zero dip axis.

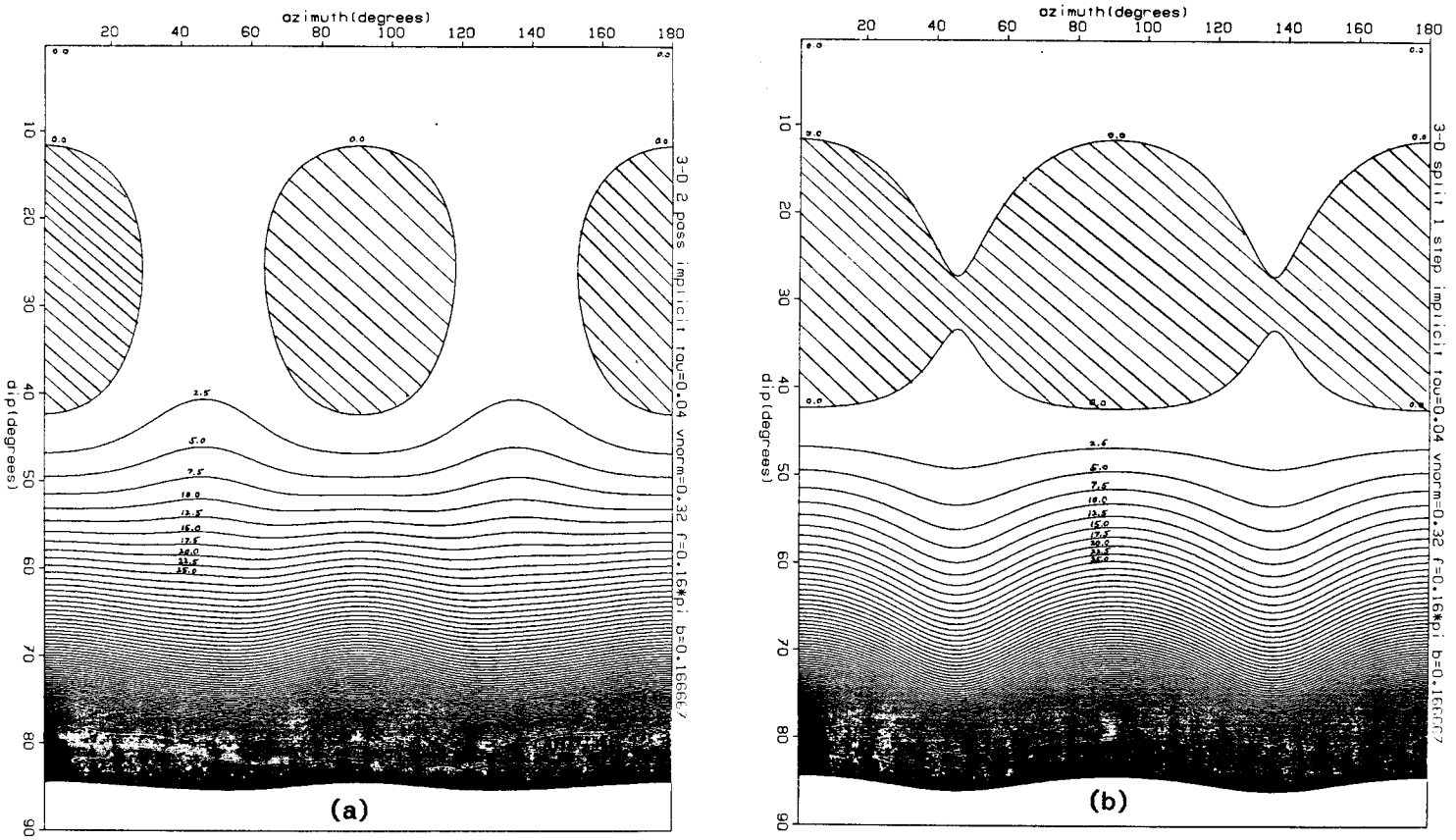

FIG. 2. Contour plot of relative phase error for the 15° implicit algorithm (with $\beta = 1/6$) using the same parameters as for Figure 1. The hatched areas are where the phase error has gone slightly negative.

Industrial strength Stolt migration

If Stolt migration is the method of preference then, as Gibson, et. al. point out, migrating the 3-D volume of data in one pass requires half the stretching and Fourier transforming operations of two-pass Stolt migration. This is no surprise as the proof of equivalence of two-pass to full 3-D constant velocity migration is simplicity itself; the first migration downshifts the frequency ω to $\hat{\omega}$ given by

$$\hat{\omega} = \left[\omega^2 - \left(\frac{v\, k_x}{2} \right)^2 \right]^{1/2} \tag{7}$$

and scales by $\hat{\omega}/\omega$. The second migration downshifts the frequency $\hat{\omega}$ to the final value k_τ given by

$$k_\tau = \left[\hat{\omega}^2 - \left(\frac{v\, k_y}{2} \right)^2 \right]^{1/2} \tag{8}$$

and scales again by $k_\tau/\hat{\omega}$. Substituting (7) into (8) gives

$$k_\tau = \left[\omega^2 - \left(\frac{v\, k_x}{2} \right)^2 - \left(\frac{v\, k_y}{2} \right)^2 \right]^{1/2} \tag{9}$$

with scale factor $k_\tau/\hat{\omega} \times \hat{\omega}/\omega = k_\tau/\omega$, exactly the frequency downshift and scale factor used in full 3-D Stolt migration.

Because the real world is not constant velocity, Stolt (1978) suggested that trace stretching be used before migration to make the section look more like a constant velocity section. More specifically, Stolt's stretching function f is designed to make the hyperbola

$$t^2 = \tau^2 + \frac{4x^2}{v^2} \tag{10}$$

look like a constant velocity hyperbola

$$f^2(t) = f^2(\tau) + \frac{4x^2}{v_o^2} \tag{11}$$

for small offset x.

Dividing (11) by (10) gives

$$\frac{f^2(t) - f^2(\tau)}{t - \tau} = (t + \tau)\, \frac{v_o^2}{v^2} \tag{12}$$

and taking the small offset limit $t \to \tau$ gives the differential equation

$$\frac{d}{d\tau} \left[f^2(\tau) \right] = 2\tau \frac{v_o^2}{v^2} \tag{13}$$

for the Stolt stretch.

After the stretching is done, migration proceeds as in the constant velocity case with the addition of one extra parameter s in the frequency mapping

$$k_\tau = \left(1 - \frac{1}{s}\right) \omega + \frac{1}{s} \left[\omega^2 - s \left(\frac{vk}{2} \right)^2 \right]^{1/2} \tag{14}$$

and final trace unstretching. The infamous constant s is often set to ½ for migration of field data and 1 for constant velocity synthetics. We note, however, that independent of s, $k_\tau = \omega$ for $k = 0$ and so flat dips are left reassuringly unmoved.

The case $s = 1$, however, gives an interesting, albeit incomplete, insight into the performance of Stolt stretch for nonconstant velocity. In this case, the two-pass method with trace stretching does give identical results to the one pass method with trace stretching. We know, however, that two-pass migration will differ from full 3-D migration for nonconstant velocity. Thus, for three dimensional datasets, the inaccuracies of Stolt stretch are virtually

the same as those arising in two pass migration.

REFERENCES

Brown, D.L., 1983, Applications of operator separation in reflection seismology, Geophysics v.48, p. 288-294.

Gibson, B., Larner, K. and Levin, S., 1983, Efficient 3-D migration in two steps, Geophys. Prosp., v. 31, p. 1-33.

Jakubowicz, H. and Levin, S., 1983, A simple exact method of 3-D migration - theory, Geophys. Prosp., v. 31, p. 34-56.

Stolt, R.H., 1978, Migration by Fourier transform, Geophysics, v.43, p.23-48.